Constructive Quantum Interference in Single-Molecule Benzodichalcogenophene Junctions

Masoud Baghernejad[a, c], Yang Yang[a], Oday A. Al-Owaedi[b], Yves Aeschi[c], Biao-Feng Zeng[a], Zahra Murtada Abd Dawood[b], Xiaohui Li[a], Junyang Liu[a], Jia Shi[a], Silvio Decurtins[c], Shi-Xia Liu[c], Wenjing Hong*[a, c] and Colin J. Lambert*[d]*

This manuscript is dedicated to the memory of Professor Thomas Wandlowski.

Abstract: Heteroatom substitution into the cores of alternant, aromatic hydrocarbons containing only even-membered rings is attracting increasing interest as a method of tuning their electrical conductance. Here we examine the effect of heteroatom substitution into molecular cores of non-alternant hydrocarbons, containing odd-membered rings. Benzodichalcogenophene (BDC) compounds are rigid, planar π-conjugated structures, with molecular cores containing 5-membered rings fused to a 6-membered aryl ring. To probe the sensitivity or resilience of constructive quantum interference (CQI) in these non-bipartite molecular cores, two C_2-symmetric molecules (I and II) and one asymmetric molecule (III) are investigated. I (II) contains S (O) heteroatoms in each of the 5-membered rings, while III contains an S in one 5-membered ring and an O in the other. Differences in their conductances arise primarily from the longer S-C and shorter O-C bond lengths compared with the C-C bond and the associated changes in their resonance integrals. We find that although the conductance of III is significantly lower than the conductances of the others, CQI is resilient and persists in all molecules.

Introduction

When a single molecule is connected to source and drain electrodes, the electrical conductance of the resulting device is controlled by the quantum interference (QI) pattern within the molecule, created by de Broglie waves of electrons injected into the molecule by the source.[1] Stimulated by the desire to develop molecular-scale diodes,[2-4] transistors,[5,6] switches[7-10] and thermoelectric devices[11-13] with improved performance, recent effort has been devoted to exploiting such wave patterns within heterocyclic aromatic molecules. Polyaromatic hydrocarbons (PAHs) and their derivatives are particularly attractive, because they contain multiple interfering pathways, which promote QI and can be influenced by external electrostatic or electrochemical gating,[14] by varying their connectivities to external electrodes[15,16] or by heteroatom substitution.[17] When the core of a graphene-like PAH is weakly coupled to external electrodes by atoms *i* and *j*, the single-molecule electrical conductance σ_{ii} depends on the choice of connecting atoms *i*, *j*.[1] Furthermore, unless a molecule is electrostatically or electrochemically gated, the highest occupied and lowest unoccupied molecular orbitals (HOMO and LUMO, respectively) levels adjust themselves such that the Fermi energy of the electrodes lies in the vicinity of the middle of the HOMO-LUMO gap.[18,19] Consequently, if the core of the molecule is weakly coupled to the electrodes (e.g., via triple bonds, which link the core to an anchoring group), the electrical conductance is proportional to $(g_{ij})^2$, where g_{ij} is the amplitude of an electronic de Broglie wave on atom j, due to electrons injected into the core at site i with energies close to the middle of the HOMO-LUMO gap. These concepts of weak coupling, connectivity and mid-gap transport have been utilised in a series of papers to develop quantum circuit rules for materials discovery and to develop a simple magic ratio rule (MRR)[15] for describing the influence of connectivity on QI in heterocyclic PAHs.

With a view to optimising transport through PAH-based molecular junctions, it is of interest to investigate how such wave patterns are modified by heteroatom substitution. If the modification is not too strong, then starting from a "parent" graphene-like PAH, such a study would allow the electrical conductance of a "daughter" heteroatom-substituted molecule to be predicted using simple perturbation theory. For bipartite, aromatic, parental cores, in which odd-numbered sites are connected to even-numbered sites only, a recent study revealed simple rules governing the effect of heteroatom substitution, which were verified by comparison with density functional theory and by experiments on heteroatom-substituted oligo(phenylene-ethynylene) compounds.[17,20]

Our aim is to investigate the effect of heteroatom substitution when the parent is a non-bipartite, aromatic molecule, stimulated in part by a desire to understand electron transport through benzodichalcogenophene (BDC) compounds, which possess a rigid and planar π-conjugated structure with strong electron donating ability.[21,22] These properties have led to their use as organo-electronic compounds in dye-sensitized solar cells (DSSC), field effect transistors (OFET), organic light-

[a] Dr. Masoud Baghernejad, Dr. Yang Yang, Dr. Biao-Feng Zeng, Dr. Xiaohui Li, Junyang Liu, Dr. Jia Shi, Prof. Wenjing Hong.
State Key Laboratory of Physical Chemistry of Solid Surfaces, Pen-Tung Sah Institute of Micro-Nano Science and Technology, College of Chemistry and Chemical Engineering, iChEM, Xiamen University, 361005, Xiamen, China
E-mail: whong@xmu.edu.cn

[b] Dr. *Oday A. Al-Owaedi, Zahra Murtada Abd Dawood*
Department of Laser Physics, Women Faculty of Science, the University of Babylon, Hilla 51001, Iraq.
E-mail: oday.alowaedi@gmail.com

[c] Dr. Masoud Baghernejad, Dr. Yves Aeschi, Prof. Wenjing Hong, Prof. Silvio Decurtins, Dr. Shi-Xia Liu.
Department of Chemistry and Biochemistry, University of Bern, Freiestrasse 3, 3012 Bern, Switzerland.
Email: liu@dcb.unibe.ch

[d] Prof. Colin J. Lambert.
Department of Physics, University of Lancaster, Lancaster, LA1 4YB, UK.
Email: c.lambert@lancaster.ac.uk

emitting diodes (OLED) and in charge transport studies of single molecules.[23-29] However the non-bipartite nature of the central core, the non-uniform bonding geometry and structural rearrangement of typical anchoring groups in the junction, complicates the interpretation of charge transport data. Improvement has been achieved through the use of alternative and rather high conductance carbon-gold anchoring using trimethylsilyl-terminated compounds, which facilitate a rather more robust data interpretation.[30,31] However, the role of QI within the non-bipartite, aromatic core has not been extensively addressed.

In the present paper, charge transport properties of three BDC compounds **I (SS)**, **II (OO)** and **III (SO)** (Figure 1) have been investigated using a scanning tunneling microscopy-break junction (STM-BJ). These molecules allow us to examine the relative effect of C_2-symmetric and asymmetric chalcogen substitution in BDC-compounds. We demonstrate that although all of them exhibit constructive quantum interference (CQI), the asymmetric **III (SO)** has a conductance value several times lower than those of the symmetric **I (SS)** and **II (OO)**. These experimental results are verified by a combination of density functional theory (DFT), tight binding (Hückel) modelling and perturbation theory.

Results and Discussion

The target compounds **I-III** were prepared according to literature methods.[21] Their charge transport properties were investigated using STM-BJ techniques,[32] as sketched in Figure 1.

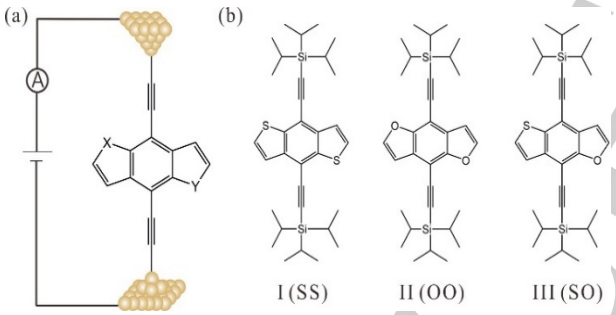

Figure 1. (a) Schematics of STM-BJ measurement. (b) Chemical structures of compounds **I (SS)**, **II (OO)**, and **III (SO)**.

As shown in Figure 2a-c, the typical conductance-distance traces (in units of the conductance quantum $G_0 = 2e^2/h$) from the conductance measurements of BDC-molecules show a well-defined plateau in the range of $\log(G/G_0)$ around -3.6 for compounds **I (SS)** and **II (OO)**, and around -3.9 for compound **III (SO),** which we assign to the conductance of single-molecule junctions. The two-dimensional (2D) conductance histograms (Figure 2d-f) show features of gold atomic contacts around $G \geq 1$ G_0 followed by a cloud-like plateau in the range [$10^{-4.6}$ $G_0 < G <$ $10^{-3.2}$ G_0], centered at $G = 10^{-3.9}$ G_0 for compound **III (SO)** and $G = 10^{-3.6}$ G_0 for compounds **I (SS)** and **II (OO)**.

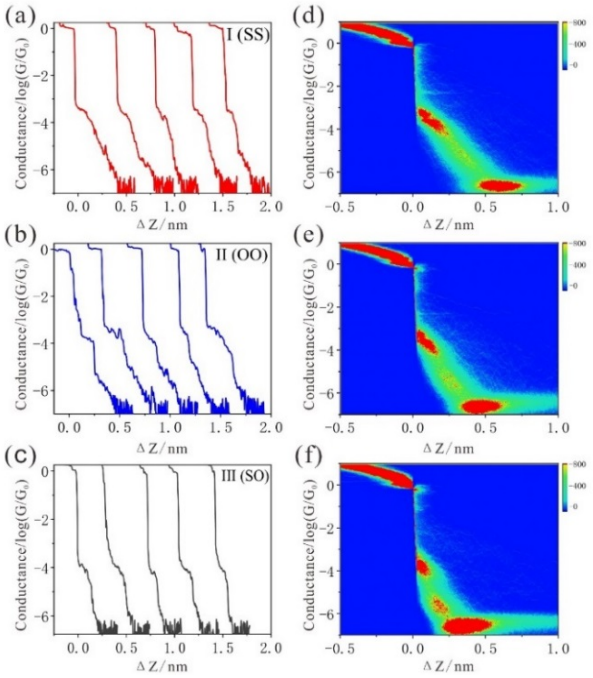

Figure 2. (a-c) Typical conductance-distance traces and (d-f) two-dimensional histograms of compounds **I (SS)**, **II (OO)**, and **III (SO)**. The histograms are constructed from more than 4000 single current-distance traces without data selection.

The cloud-like plateau in 2D histogram leads to the peak in the one-dimensional (1D) conductance histogram that constructed form more than 4000 individual traces without any data selection, as shown in Figure 3. This is attributed to the formation of single-molecule junction. As shown by our theoretical modelling below, this trend in conductances is a reflection of the fact that the LUMO orbitals of compounds **I (SS)** and **II (OO)** are shifted to lower and higher energies respectively relative to compound **III (SO)**. In addition, the lengths of the S-C and O-C bonds are $L_{S\text{-}C}$ = 0.174 nm and $L_{O\text{-}C}$ = 0.136 nm, which are longer and shorter respectively than the length of the C-C bond ($L_{C\text{-}C}$=0.144 nm), leading to smaller and larger resonance integrals between the heteroatoms on their neighboring carbons. Our theoretical modelling reveals that the latter effect rather than the level shift of the LUMOs leads to the lower conductance of compound **III (SO)** compared with compounds **I (SS)** and **II (OO)**.

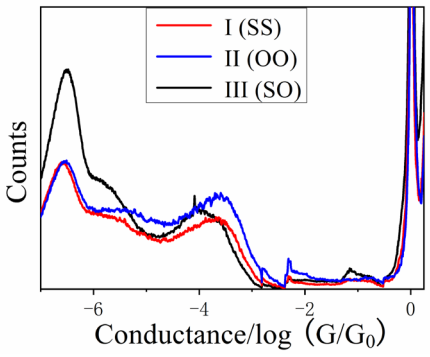

Figure 3. One-dimensional conductance histograms of compounds **I (SS)**, **II (OO)**, and **III (SO)**.

To better understand the conductance behavior, the electronic properties of the molecules and electrical behavior of the junctions were investigated using DFT-based theory and tight-binding methods.[33] Initial studies of the electronic structures of all molecules were carried out at B3LYP level of theory [34] with 6-31G**[3] basis set. Figure 4 gives the plots of the HOMOs and LUMOs. These orbitals are real functions and have either a positive or negative [35,36] sign. Crucially, the sign of the HOMOs on the left acetylene linker are of opposite to the sign on the right acetylene linker, whereas the LUMOs have the same sign on the left and right acetylene linkers. As discussed previously,[35] this means that for each molecule, the HOMO orbital product is negative and the LUMO orbital product is positive. Therefore, their inter-orbital quantum interference is constructive within the HOMO-LUMO gap. Figure 4 shows that the HOMOs of all molecules are extended over the BDC backbone. The LUMOs exhibit a negligible weight on the S or O atoms and are therefore are less delocalized than the HOMOs. In both cases, there is negligible electron density on the triisopropylsilyl (TIPS) groups.

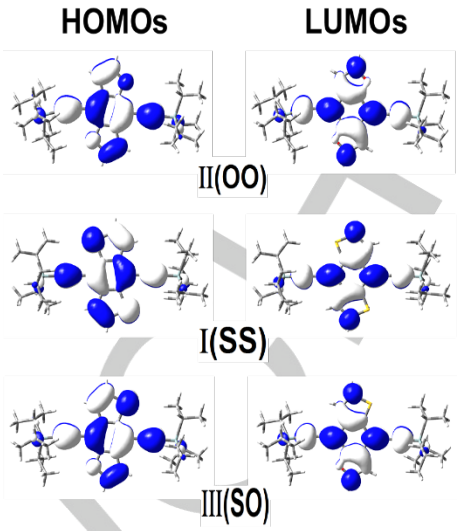

Figure 4. Plots of the HOMO and LUMO of all molecules (iso-surfaces ±0.02 $(e/bohr^3)^{1/2}$).

Figure 5a shows the relaxed geometries of the molecules within the gold junctions and Figure 5b shows their corresponding transmission coefficients. As expected from Hückel theory (see Supporting Information), the LUMO transmission resonances (near E = 2.3 eV) of the II (OO) and I (SS) molecules respectively lie above and below that of the III (SO) molecule. Furthermore, as expected, since the HOMO and LUMO orbital products are of opposite sign, interference is constructive[35] and there is no destructive interference feature within the gap. A key factor governing the conductance of a molecular junction is the position of the Fermi level of a metal electrode with respect to the molecular HOMO and LUMO levels. In turn this energy alignment is sensitive to the chemical nature of the contacting groups, which binds the molecule to the electrode, and also the precise configuration of the metal electrode-molecule contact.[37-39] However, it is well-known that the Fermi energy predicted by DFT is often not reliable, and as such the room temperature electrical conductance G was computed for a range of Fermi energies E_F; the calculated G is plotted as a function of $E_F - E_F^{DFT}$ in Figure 5b. This multi-point fitting of the Fermi energy is a commonly accepted procedure in DFT-based calculations in molecular electronics.[40-42] To determine E_F, the predicted conductance values of all molecules were compared with the experimental values and a single common value of E_F was chosen, which gave the closest overall agreement. This yielded a value of $E_F - E_F^{DFT}$ = 1.0 eV, which is used in all of the DFT results described below. The experimental data now is interpreted with the aid of Figure 5b, which indicates that in all cases the Fermi level lies close to the middle of the HOMO-LUMO gap and transport takes place via non-resonant tunneling.[43-45] Table 1 shows a comparison between experimental and theoretical conductances, along with other relevant junction parameters.

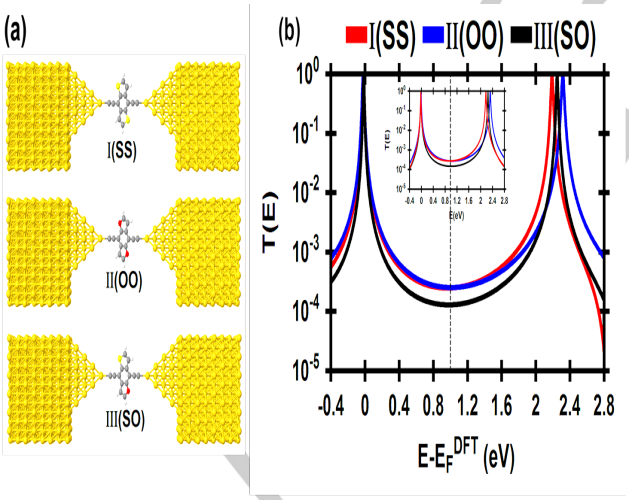

Figure 5. (a) The relaxed geometries of molecular junctions of **I (SS)**, **II (OO)**, and **III (SO)**. (b) The transmission functions for all molecular junctions. Black dashed line shows the chosen Fermi energy ($E_F - E_F^{DFT}$ = 1 eV). The insert shows the result of a tight binding calculation (see Supporting Information) based on a minimal Hückel description of transport through the cores of the molecules.

Table 1. The experimental (Exp. G/G_0) and calculated conductance values (Th. G/G_0) at $E - E_F^{DFT}$ = 1.0 eV. The calculated electrode separation in relaxed junctions (Z); Z = $d_{Au\text{-}Au}$ - 0.25 nm, where 0.25 nm is the calculated center-to-center distance of the apex atoms of the two opposing gold pyramids when the conductance equals G_0 in the absence of a molecule. $d_{Au\text{-}Au}$ is the calculated center-to-center distance of the apex atoms of the two opposing gold pyramids in relaxed junctions. Molecular length (d) is the distance between the centres of anchor atoms in relaxed junction. Bond length (X) is the distance between the top gold atoms of the pyramids and the anchor atoms in relaxed junctions. ΔE (eV) is the biding energy of the molecules to the electrodes.

Molecule	Exp. G/G_0	Th. G/G_0	Z nm	$d_{Au\text{-}Au}$ nm	d nm	X nm	ΔE (eV)
SS	2.512×10^{-4}	2.528×10^{-4}	0.991	1.241	0.817	0.212	-3.3
OO	2.512×10^{-4}	2.528×10^{-4}	0.994	1.244	0.821	0.212	-3.4
SO	1.258×10^{-4}	1.291×10^{-4}	0.992	1.242	0.819	0.212	-3.02

To understand the relative effect of the S and O heteroatoms, we constructed a minimal tight-binding (Hückel) representation of the "parental" core of the molecules before heteroatom substitution shown in Figure 6 and then considered the effect of heteroatom substitution to yield the "daughters" shown in Figure 5a. The simplest tight-binding Hamiltonian of the parent is obtained by assigning a site energy ε_0 to each diagonal and a nearest neighbor hopping integral $-\gamma$ between neighbouring sites, i.e., $H_{ii} = \varepsilon_0$ and $H_{ij} = -\gamma$ if i,j are nearest neighbours. A minimal model of the heteroatom-substituted "daughters" is then obtained simply by shifting the site energies of sites 3 and 9 to accommodate the different electronegativities of O and S, leading to first-order shifts in their LUMOs and a negligible shift in their HOMOs (see SI for a detailed analysis). However, as shown in Figure S3 of the SI, such shifts alone are not sufficient to yield agreement with the DFT results and experiments, and would not yield a lower value of conductance for the asymmetric molecule. On the other hand, if the O-C and S-C hopping integrals are adjusted to account for the differences in lengths between the O-C bond (0.136 nm), the S-C bond (0.174 nm) compared with the C-C bonds (0.144 nm), then excellent agreement between the tight-bonding model (see insert in Figure 5b) and DFT (main part of Figure 5b) is obtained. This demonstrates that longer S-C and shorter O-C bonds lengths compared with the C-C bond and the associated changes in their resonance integrals leads to the lower conductance of **III (SO)** compared with **I (SS)** and **II (OO)**.

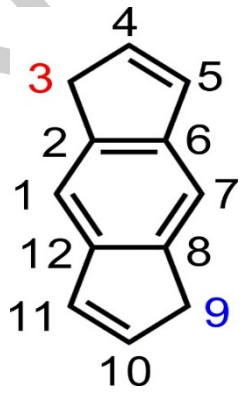

Figure 6. A tight binding representation of the isolated core of the benzodichalcogenophene molecule, with nearest neighbour coupling elements and on-site energies adjusted to account for the presence of heteroatoms on sites 3 and 9.

Conclusions

In conclusion, we have carried out a combined experimental and theoretical study of the role of heteroatoms on electron transport through asymmetric and symmetric alkyne-terminated benzodichalcogenophene compounds. Excellent agreement between experiments, DFT-based theory and a minimal tight binding model is obtained. The tight-binding modelling of heteroatom substitution in these non-bipartite cores demonstrates that the lower conductance of the asymmetric molecule arises from the asymmetry induced by different bond lengths in the two 5-membered rings of the molecule.

Furthermore, as shown in Figure 4, the HOMO and LUMO orbital products of all molecules are of opposite sign and therefore, as confirmed by the absence of a destructive interference dip in their DFT transmission functions (Figure 5), their inter-orbital quantum interference is constructive [35] and is resilient to heteroatom substitution.

Experimental Section

The STM-BJ measurements were carried out with a Molecular Imaging PicoSPM housed in an all-glass argon-filled chamber and equipped with a dual preamplifier capable of recording currents in a wide range of 1 pA to 150 μA with high resolution. The non-amplified low-current signal was fed back to the STM controller preserving the STM imaging capability. The current-distance measurements were performed with a separate, lab-build analog ramp unit. For further technical details we refer to our previous work[46,47]. The sample electrode was gold single crystal bead. The Au (polycrystalline) facet prior to each experiment was subjected to electrochemical polishing and annealing in a hydrogen flame followed by cooling under Ar. A freshly prepared solution containing typically 0.1 mM of the respective molecule was added to a Kel-F flow-through liquid cell mounted on top of the sample and the uncoated STM tip was electrochemically etched using gold wire (Goodfellow, 99.999%, 0.25 mm diameter) capable of imaging with atomic resolution. This system relies on trapping a molecule between the end of an Au tip and the gold substrate.

After assembling the experiment, the following protocols were applied: The tip was brought to a preset tunneling position typically defined by iT = 50 to 100 pA and a bias voltage Vbias = 0.10 V, followed by imaging the substrate. After fixing the lateral position of the tip, the STM feedback is switched off and current-distance measurements were performed and then the vertical movement of the tip controlled by the ramp unit. The measuring cycle was performed in the following way: The controlling software drives the tip towards the adsorbate-modified surface. The approach was stopped until a predefined upper current limit was reached (typically 10 μA or < 10 G0 with G0 being the fundamental conductance quantum 77.5 μS). After a short delay (~100 ms) ensuring tip relaxation and the formation of stable contacts, the tip was retracted by 2 to 5 nm until a low current limit of ~10 pA was reached. The approaching and withdrawing rates were varied from 56 to145 nm/s. The entire current-distance traces were recorded with a digital oscilloscope (Yokogawa DL 750, 16 bit, 1 MHz sampling frequency) in blocks of 186 individual traces. Up to 4000 traces were recorded for each set of experimental conditions to guarantee the statistical significance of the results.

Theoretical Section

Initial studies of the electronic structures of all molecules were carried out at B3LYP level of theory with 6-31G^{**3} basis set. Plots of the highest occupied and lowest unoccupied molecular orbitals (HOMO and LUMO, respectively) are shown in Figure 4.

To provide further insight into the experimentally observed trends, and to better evaluate the properties and behavior of these molecular junctions, calculations using a combination of DFT (the SIESTA code)[48] and a non-equilibrium Green's function formalism were also carried out. The DFT-Landauer approach used in the modeling assumes that on the time scale taken by an electron to traverse the molecule, inelastic scattering is negligible. This is known to be an accurate assumption for molecules up to several nanometers in length.

For the transport calculations, each molecule was attached to opposing 35-atom (111) directed pyramidal gold electrodes, then geometrically optimization were carried out using the DFT code SIESTA, with a generalized gradient approximation[48,49] (PBE functional), double ζ polarized basis set, 0.01 eV/A force tolerance, a real-space grid with a plane wave cut-off energy of 250 Ry, zero bias voltage and 1 k points. The molecules and first layers of gold atoms within each electrode were then allowed to relax, to yield the optimal junction geometries. Then, eight layers of (111)-oriented bulk gold with each layer consisting of 6×6 atoms and a layer spacing of 0.235 nm were used to create the molecular junctions as shown in Figure 5(a). These layers were then further repeated to yield infinitely-long current-carrying gold electrodes. From these model junctions the transmission coefficient, *T(E)*, was calculated using the GOLLUM code.[33] To determine E_F, the predicted conductance values of all molecules were compared with the experimental values and a single common value of E_F was chosen, which gave the closest overall agreement. This yielded a value of $E_F - E_F^{DFT}$ = 1.0 eV, which is close to the middle of the HOMO-LUMO gap and has been used in all of the theoretical results described previously. The employment of DFT to compute the ground state energy of various molecular junctions, permits to calculate binding energies and optimal geometries. However, these calculations are subject to errors, due to the employing of localized basis sets, which are concentrated on the nuclei. At the point when atoms are sufficiently close to each other so that their basis functions will overlap. This might cause an artificial strengthening of the atomic interaction and an artificial shortening of the atomic distances and hence this could influence the aggregate energy of the system. The solution of this kind of errors has been demonstrated by the basis set superposition error correction (BSSE)[50] or the counterpoise correction.[51] Assuming two molecular systems, denoted a and b, the energy of the interaction may be expressed as:

$$\Delta E(ab) = E_{ab} - (E_a^{ab} + E_b^{ab})$$

The total energy of the combined *a* and *b* system is E_{ab}, while the total energies of isolated systems *a* and *b* are E_a and E_b respectively with keeping identical basis sets for the three energies. ΔE_{ab} is the binding energy between anchor groups and gold electrode.

Acknowledgements

We thank the National Natural Science Foundation of China (21503179, 21673195, 21722305,21703188), the National Key R&D Program of China (2017YFA0204902), the Fundamental Research Funds for the Central Universities (Xiamen University: 20720170035) for funding work in Xiamen. Support from the UK EPSRC is acknowledged, through grant nos. EP/N017188/1, EP/P027156/1 and EP/N03337X/1. Support from the European Commission is provided by the FET Open project 767187 – QuIET and the H2020 project Bac-To-Fuel. Support from the Iraqi Ministry of Higher Education and Scientific Research.

Keywords: quantum interference • single-molecule conductors • density functional theory • scanning tunneling microscopy • perturbation theory.

References

[1] Lambert, C. J. Chem. Soc. Rev. 2015, 44, 875-888.
[2] Díez-Pérez, I.; Hihath, J.; Lee, Y.; Yu, L.; Adamska, L.; Kozhushner, M. A.; Oleynik, I. I.; Tao, N. Nat Chem 2009, 1, 635-641.
[3] Yuan, L.; Breuer, R.; Jiang, L.; Schmittel, M.; Nijhuis, C. A. Nano Lett. 2015, 15, 5506-5512.
[4] Batra, A.; Darancet, P.; Chen, Q. S.; Meisner, J. S.; Widawsky, J. R.; Neaton, J. B.; Nuckolls, C.; Venkataraman, L. Nano Lett. 2013, 13, 6233-6237.
[5] Xu, B.; Xiao, X.; Yang, X.; Zang, L.; Tao, N. J. Am. Chem. Soc. 2005, 127, 2386-2387.
[6] Song, H.; Kim, Y.; Jang, Y. H.; Jeong, H.; Reed, M. A.; Lee, T. Nature 2009, 462, 1039-1043.
[7] Blum, A. S.; Kushmerick, J. G.; Long, D. P.; Patterson, C. H.; Yang, J. C.; Henderson, J. C.; Yao, Y.; Tour, J. M.; Shashidhar, R.; Ratna, B. R. Nat. Mater. 2005, 4, 167-172.
[8] van der Molen, S. J.; Liao, J.; Kudernac, T.; Agustsson, J. S.; Bernard, L.; Calame, M.; van Wees, B. J.; Feringa, B. L.; Schönenberger, C. S. Nano Lett. 2009, 9, 76-80.
[9] Jia, C. C.; Migliore, A.; Xin, N.; Huang, S. Y.; Wang, J. Y.; Yang, Q.; Wang, S. P.; Chen, H. L.; Wang, D. M.; Feng, B. Y.; Liu, Z. R.; Zhang, G. Y.; Qu, D. H.; Tian, H.; Ratner, M. A.; Xu, H. Q.; Nitzan, A.; Guo, X. F. Science 2016, 352, 1443-1445.
[10] Frisenda, R.; Harzmann, G. D.; Celis Gil, J. A.; Thijssen, J. M.; Mayor, M.; van der Zant, H. S. J. Nano Lett. 2016, 16, 4733-4737.
[11] Rincon-Garcia, L.; Ismael, A. K.; Evangeli, C.; Grace, I.; Rubio-Bollinger, G.; Porfyrakis, K.; Agrait, N.; Lambert, C. J. Nat. Mater. 2016, 15, 289-293.
[12] Sadeghi, H.; Sangtarash, S.; Lambert, C. J. Nano Lett. 2015, 15, 7467-7472.
(13) Kim, Y.; Jeong, W.; Kim, K.; Lee, W.; Reddy, P. Nat. Nanotechnol. 2014, 9, 881-885.
[14] Baghernejad, M.; Zhao, X.; Baruel Ornso, K.; Fueg, M.; Moreno-Garcia, P.; Rudnev, A. V.; Kaliginedi, V.; Vesztergom, S.; Huang, C.; Hong, W.; Broekmann, P.; Wandlowski, T.; Thygesen, K. S.; Bryce, M. R. J. Am. Chem. Soc. 2014, 136, 17922-17925.
[15] Geng, Y.; Sangtarash, S.; Huang, C.; Sadeghi, H.; Fu, Y.; Hong, W.; Wandlowski, T.; Decurtins, S.; Lambert, C. J.; Liu, S. X. J. Am. Chem. Soc. 2015, 137, 4469-4476.; Sangtarash, S.; Huang, C.; Sadeghi, H.; Sorohhov, G.; Hauser, J.; Wandlowski, T.; Hong, W.; Decurtins, S.; Liu, S-X.; Lambert, C.J.; Journal of the American Chemical Society 137 (35), 11425-11431 (2015)
[16] Yang, G.; Wu, H.; Wei, J.; Zheng, J.; Chen, Z.; Liu, J.; Shi, J.; Yang, Y.; Hong, W. Chin. Chem. Lett. 2018, 29, 147-150.
[17] Liu, X.; Sangtarash, S.; Reber, D.; Zhang, D.; Sadeghi, H.; Shi, J.; Xiao, Z.-Y.; Hong, W.; Lambert, C. J.; Liu, S.-X. Angew. Chem. Int. Ed. 2017, 56, 173-176.
[18] Yang, Y.; Liu, J. Y.; Yan, R. W.; Wu, D. Y.; Tian, Z. Q. Chemical Journal of Chinese Universities-Chinese 2015, 36, 9-23.
[19] Manrique, D. Z.; Huang, C.; Baghernejad, M.; Zhao, X.; Al-Owaedi, O. A.; Sadeghi, H.; Kaliginedi, V.; Hong, W.; Gulcur, M.; Wandlowski, T.; Bryce, M. R.; Lambert, C. J. Nat. Commun. 2015, 6, 6389.
[20] Sangtarash, S.; Sadeghi, H.; Lambert, C. J. Nanoscale 2016, 8, 13199-13205.
[21] Aeschi, Y.; Li, H.; Cao, Z.; Chen, S.; Amacher, A.; Bieri, N.; Oezen, B.; Hauser, J.; Decurtins, S.; Tan, S.; Liu, S.-X. Org. Lett. 2013, 15, 5586-5589.
[22] Yi, C. Y.; Blum, C.; Lehmann, M.; Keller, S.; Liu, S. X.; Frei, G.; Neels, A.; Hauser, J.; Schürch, S.; Decurtins, S. J. Org. Chem. 2010, 75, 3350-3357.

[23] Didane, Y.; Mehl, G. H.; Kumagai, A.; Yoshimoto, N.; Videlot-Ackermann, C.; Brisset, H. J. Am. Chem. Soc. 2008, 130, 17681–17683.
[24] Chen, H.-Y.; Hou, J.; Zhang, S.; Liang, Y.; Yang, G.; Yang, Y.; Yu, L.; Wu, Y.; Li, G. Nat. Photonics 2009, 3, 649-653.
[25] Li, H.; Jiang, P.; Yi, C.; Li, C.; Liu, S.-X.; Tan, S.; Zhao, B.; Braun, J.; Meier, W.; Wandlowski, T.; Decurtins, S. Macromolecules 2010, 43, 8058-8062.
[26] Zhou, J.; Wan, X.; Liu, Y.; Zuo, Y.; Li, Z.; He, G.; Long, G.; Ni, W.; Li, C.; Su, X.; Chen, Y. J. Am. Chem. Soc. 2012, 134, 16345-16351.
[27] Li, Z.; Li, H.; Chen, S.; Froehlich, T.; Yi, C.; Schonenberger, C.; Calame, M.; Decurtins, S.; Liu, S.-X.; Borguet, E. J. Am. Chem. Soc. 2014, 136, 8867-8870.
[28] Li, H.; Yi, C.; Moussi, S.; Liu, S.-X.; Daul, C.; Graetzel, M.; Decurtins, S. RSC Adv. 2013, 3, 19798-19801
[29] Li, H.; Tang, P.; Zhao, Y.; Liu, S.-X.; Aeschi, Y.; Deng, L.; Braun, J.; Zhao, B.; Liu, Y.; Tan, S.; Meier, W.; Decurtins, S. J. Polym. Sci. Part A: Polym Chem, 2012, 50, 2935-2943.
[30] Cheng, Z. L.; Skouta, R.; Vazquez, H.; Widawsky, J. R.; Schneebeli, S.; Chen, W.; Hybertsen, M. S.; Breslow, R.; Venkataraman, L. Nat. Nanotechnol. 2011, 6, 353-357.
[31] Hong, W.; Li, H.; Liu, S.-X.; Fu, Y.; Li, J.; Kaliginedi, V.; Decurtins, S.; Wandlowski, T. J. Am. Chem. Soc. 2012, 134, 19425-19431.
[32] Xu, B.; Tao, N. J. Science 2003, 301, 1221-1223.

[33] Ferrer, J.; Lambert, C. J.; García-Suárez, V. M.; Manrique, D. Z.; Visontai, D.; Oroszlany, L.; Rodríguez-Ferradás, R.; Grace, I.; Bailey, S. W. D.; Gillemot, K.; Sadeghi, H.; Algharagholy, L. A. New J. Phys. 2014, 16, 093029.
[34] Becke, A. D. J. Chem. Phys. 1993, 98, 5648-5652.
[35] Lambert, C. J.; Liu, S.-X. Chem. Eur. J. 2018, 24, 4193-4201.
[36] Stadler, R.; Jacobsen, K. W. Phys. Rev. B 2006, 74, 161405.
[37] Al-Owaedi, O. A.; Milan, D. C.; Oerthel, M.-C.; Bock, S.; Yufit, D. S.; Howard, J. A. K.; Higgins, S. J.; Nichols, R. J.; Lambert, C. J.; Bryce, M. R.; Low, P. J. Organometallics 2016, 35, 2944-2954.
[38] Yang, Y.; Liu, J.; Feng, S.; Wen, H.; Tian, J.; Zheng, J.; Schöllhorn, B.; Amatore, C.; Chen, Z.; Tian, Z. Nano Res. 2016, 9, 560-570.
[39] Markussen, T.; Settnes, M.; Thygesen, K. S. J. Chem. Phys. 2011, 135, 144104
[40] Milan, D. C.; Al-Owaedi, O. A.; Oerthel, M.-C.; Marqués-González, S.; Brooke, R. J.; Bryce, M. R.; Cea, P.; Ferrer, J.; Higgins, S. J.; Lambert, C. J.; Low, P. J.; Manrique, D. Z.; Martin, S.; Nichols, R. J.; Schwarzacher, W.; García-Suárez, V. M. J. Phys. Chem. C 2015, 120, 15666-15674.
[41] Schwarz, F.; Kastlunger, G.; Lissel, F.; Riel, H.; Venkatesan, K.; Berke, H.; Stadler, R.; Lortscher, E. Nano Lett. 2014, 14, 5932-5940.
[42] Sugimoto, K.; Tanaka, Y.; Fujii, S.; Tada, T.; Kiguchi, M.; Akita, M. Chem Commun (Camb) 2016, 52, 5796-5799.
[43] Adak, O., et al., Nano Letters, 2015. 15(6): p. 3716–3722.
[44] Sugimoto, K.; Tanaka, Y.; Fujii, S.; Tada, T.; Kiguchi, M.; Akita, M. Chem Commun (Camb) 2016, 52, 5796-5799.
[45] Wen, H.-M.; Yang, Y.; Zhou, X.-S.; Liu, J.-Y.; Zhang, D.-B.; Chen, Z.-B.; Wang, J.-Y.; Chen, Z.-N.; Tian, Z.-Q. Chem. Sci. 2013, 4, 2471–2477.
[46] Hong, W.; Valkenier, H.; Meszaros, G.; Manrique, D. Z.; Mishchenko, A.; Putz, A.; Garcia, P. M.; Lambert, C. J.; Hummelen, J. C.; Wandlowski, T. Beilstein J. Nanotechnol. 2011, 2, 699-713.
[47] Yang, Y.; Gantenbein, M.; Alqorashi, A.; Wei, J.; Sangtarash, S.; Hu, D.; Sadeghi, H.; Zhang, R.; Pi, J.; Chen, L.; Huang, X.; Li, R.; Liu, J.; Shi, J.; Hong, W.; Lambert, C. J.; Bryce, M. R. J. Phys. Chem. C 2018, 122, 14965-14970.
[48] Soler, J. e. M.; Artacho, E.; Gale, J. D.; Garc´ıa, A.; Junquera, J.; Ordej´on, P.; S´anchez-Portal, D. J. Phys-Condens. Mat. 2002, 14, 2745–2779.
[49] Artacho, E.; Anglada, E.; Dieguez, O.; Gale, J. D.; Garcia, A.; Junquera, J.; Martin, R. M.; Ordejon, P.; Pruneda, J. M.; Sanchez-Portal, D.; Soler, J. M. J. Phys-Condens. Mat. 2008, 20, 064208.
[50] Jansen, H. B.; Ros, P. Chem. Phys. Lett. 1969, 3, 140-143.
[51] Boys, S. F.; Bernardi, F. Mol. Phys. 1970, 19, 553-566.

Entry for the Table of Contents (Please choose one layout)

Layout 1:

FULL PAPER

Text for Table of Contents

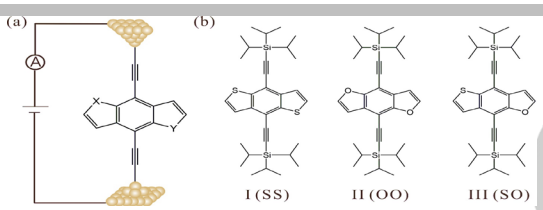

Masoud Baghernejad[a, c], Yang Yang#[a], Oday A. Al-Owaedi#[b], Yves Aeschi[c], Biao-Feng Zeng[a], Zahra Murtada Abd Dawood[b], Xiaohui Li[a], Junyang Liu[a], Jia Shi[a], Silvio Decurtins[c], Shi-Xia Liu[c], Wenjing Hong*[a, c] and Colin J. Lambert*[d]*

Page No. 1– Page No.6

Constructive Quantum Interference in Single-Molecule Benzodichalcogenophene